Three-Dimensional Quantitative Structure−Activity Relationship Studies on Selected MT_1 and MT_2 Melatonin Receptor Ligands: Requirements for Subtype Selectivity and Intrinsic Activity Modulation

Silvia Rivara,*,† Marco Mor,† Claudia Silva,† Valentina Zuliani,† Federica Vacondio,† Gilberto Spadoni,‡ Annalida Bedini,‡ Giorgio Tarzia,‡ Valeria Lucini,§ Marilou Pannacci,§ Franco Fraschini,§ and Pier Vincenzo Plazzi†

Dipartimento Farmaceutico, Università degli Studi di Parma, Parco Area delle Scienze 27/A, I-43100 Parma, Italy, Istituto di Chimica Farmaceutica e Tossicologica, Università degli Studi di Urbino, Piazza Rinascimento 6, I-61029 Urbino, Italy, and Cattedra di Chemioterapia, Dipartimento di Farmacologia, Università degli Studi di Milano, Via Vanvitelli 32, I-20129 Milano, Italy

Received July 5, 2002

The three-dimensional quantitative structure−activity relationship comparative molecular field analysis (3D-QSAR CoMFA) approach was applied to some classes of melatonin (MLT) membrane receptor ligands, with the principal aim of exploring the correlation between their steric features and MT_2-selective antagonism. Binding data obtained from cloned MT_1 and MT_2 receptor subtypes were used to develop 3D-QSAR models for agonists and for antagonists at the two receptor subtypes, looking for the structural requirements for receptor subtype selectivity. In particular, we superposed the compounds showing antagonist activity, or very low intrinsic activity at the GTPγS test, following the hypothesis that the occupation of an additional pocket positioned out of the plane of MLT is one of the major determinants for MT_2 selectivity; the statistical models obtained confirmed this hypothesis. Structure−intrinsic activity relationship studies, applied to a set of compounds homogeneously tested, allowed the identification of the structural features whose modulation shifts the behavior from that of the agonist to that of the antagonist. The pocket out of the plane of MLT was identified as one of the key features for obtaining selective MT_2 antagonists. The reliability of our statistical models was further confirmed by the correct prediction of the pharmacological behavior of some N-substituted melatonin derivatives, which were prepared and tested on cloned receptor subtypes.

Introduction

Since the first report on the ability of melatonin (MLT, *N*-acetyl-5-methoxytryptamine) to induce pigment aggregation in the skin of frogs, considerable knowledge has been gained on its role and its mechanisms of action, although we are still a long way from a complete and exhaustive understanding.

MLT is an indole-derived neurohormone mainly secreted by the pineal gland with a circadian rhythm, its synthesis and release being stimulated by darkness. MLT exerts a variety of effects, influencing the sleep−wake cycle and the entrainment of the circadian rhythms,[1,2] reproduction,[3] the cardiovascular[4,5] and the digestive systems,[6] and retinal physiology. For this reason, different putative pharmacological applications have been proposed for MLT and its analogues, mainly for the treatment of circadian rhythm disturbances but also in other fields, such as migraine headaches and seasonal depression.[7−9] Moreover, the antioxidant,[10] neuroprotective,[11] and immunomodulatory[12] properties of MLT are currently being investigated; they may lead to the application of MLT in important clinical fields, for example, in degenerative pathologies such as Alzheimer's disease.[13]

MLT actions are the consequence of its binding to receptors, although it also displays receptor-independent effects. In particular, MLT binds to membrane receptors, namely the MT_1 and MT_2 receptors, found in mammal tissues, and the Mel_1c receptor, which has been found in vertebrates but not in mammals. Recently, the so-called *MT_3* receptor, characterized in Syrian hamster tissues, has been recognized as the homologue of the human quinone reductase 2, an enzyme involved in detoxifying processes.[14] Moreover, nuclear receptors[15] have been reported for MLT, as well as other intracellular binding sites, such as calmodulin.[16]

MT_1 and MT_2 receptors are G protein-coupled receptors widely distributed in the human body both in the central nervous system and in peripheral tissues.[9] Despite their importance, little information is available about their pattern of interactions with ligands, the molecular basis for subtype selectivity, and their physiological role. Several authors have proposed interaction schemes between MLT and selected amino acids of the receptor, but these have only been based either on the primary sequence of the receptor cloned from the *Xenopus laevis* melanophore[17,18] or on the residues conserved in various cloned MLT receptors.[19] Site-

* To whom correspondence should be addressed. Phone: ++39 0521 905062. Fax: ++39 0521 905006. E-mail: silvia.rivara@unipr.it.
† Università degli Studi di Parma.
‡ Università degli Studi di Urbino.
§ Università degli Studi di Milano.

10.1021/jm020982d CCC: $25.00
Published on Web 03/19/2003

directed mutagenesis studies have shown that some amino acids are important for the binding of agonists and/or antagonists to the MT_1 subtype.[20−22] The application of nonselective and MT_2-selective antagonists, as well as of biotechnological methodologies, allowed for the clarification that the MT_2 receptor plays a role in entraining the circadian rhythms[23,24] and in the humoral and cellular immunity stimulated by MLT,[25] although in general the distinct role of the two subtypes is difficult to ascertain, being coexpressed on the same tissues.

The investigation into MT_1 and MT_2 ligands paralleled that into receptors, exploiting the design of new compounds and the identification of the structural requirements for receptor binding. Various classes of compounds have been synthesized by our research group[26,27] and by other authors,[28−39] and varying approaches have been applied to identify the important features for receptor interaction. In particular, pharmacophore analysis has allowed for the definition of the putative active conformation of MLT,[26,40,41] and SAR and QSAR studies have rationalized the results obtained from structure modulation.[29,36,42−45] In this context, three-dimensional quantitative structure−activity relationship (3D-QSAR) studies have provided a tridimensional depiction of the effect on potency due to the occupation of different regions of space by functional groups.[41,46,47] Most of these studies were based on biological data obtained from native tissues in which a heterogeneous population of receptor subtypes is often expressed. This hampered the study of receptor subtype selectivity until the cloning, in recent years, of the two receptors, which provided binding and pharmacological data relative to the two subtypes.[38,39,42,43,45,48−51]

Unfortunately, the majority of the compounds have exhibited scarce subtype selectivity or no selectivity at all. This is particularly true for MLT receptor agonists, while some MT_2-selective partial agonists and antagonists have been reported. Therefore, the reduced availability of selective compounds not only prevented the identification of the structural determinants for differential interaction at the two receptor subtypes but also hampered the understanding of the physiological role of each subtype.

MT_2 receptor selective ligands belong to different structural classes,[38,48,51] displaying different degrees of binding affinity and selectivity. For example, luzindole[51] (**23**) is characterized by poor binding to MT_1 and MT_2 receptors and by limited selectivity, while *N*-[(1-*p*-chlorobenzyl-4-methoxy-1*H*-indol-2-yl)methyl]propanamide[45] (**30**) displays more than 100 times the MT_2 selectivity, comparable to that of 4P-PDOT (**34**),[51] one of the best known and selective MT_2 receptor ligands known so far.

In this context, our research addressed the issue of MLT receptor selectivity, since we were interested in the definition of the structural requirements for binding to each receptor subtype. For this reason, we performed structure−affinity relationship studies on MT_1 and MT_2 receptor agonists and antagonists, which were treated separately, by means of a 3D-QSAR approach. In particular, in the field of MLT receptor antagonists, we wanted to verify if a hypothesis on selective binding to the MT_2 receptor could be validated by statistical analysis. This hypothesis, developed from the results of previous structure−activity investigations and from the analysis of the structural features of some MT_2-selective ligands,[44,45,52] is based on the presence of an additional pocket at the MT_2 receptor positioned out of the plane of the aromatic nucleus that characterizes MLT receptor ligands (the indole ring of MLT, for example). Its occupancy would increase the binding affinity at the MT_2 receptor compared to that of the MT_1, at the same time lowering the intrinsic activity of the compounds and moving toward the antagonist behavior. This pocket would not be present at the MT_1 receptor; therefore, compounds with a substituent out of the plane of the molecule are characterized by very low affinity at this receptor subtype. The compounds selected for the analysis were either synthesized by us or taken from the literature among those whose affinity data at the two cloned receptor subtypes and intrinsic activity values were available (Tables 1 and 2). Moreover, for a set of compounds (Table 3) whose intrinsic activity had been homogeneously evaluated by means of the GTPγS test, we investigated structure−intrinsic activity relationships, looking for the features that characterize agonist and antagonist behavior, at both receptor subtypes.

Table 1. Experimental and Calculated Relative Binding Affinity (pRA) at MT_1 and MT_2 Receptors for Agonists

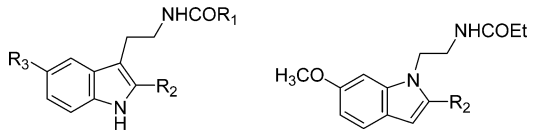

1-10

11-13

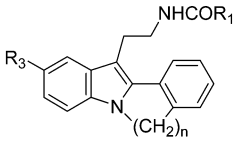

14-22

compd	R_1	R_2	R_3	*n*	pRA_1 (MT_1)	pRA_2 (MT_2)	ref	pRA_1 calcd[a]	pRA_2 calcd[b]
1 (MLT)	Me	H	OMe		0	0		−0.03	−0.17
2	Me	Br	OMe		0.91	0.51	44	1.04	0.63
3	Me	I	OMe		1.01	0.86	44	1.17	0.8
4	Me	Ph	OMe		1.03	0.99	44	0.95	1.18
5	Et	H	OMe		0.40	−0.04	42	−0.11	−0.26
6	Pr	H	OMe		0.16	−0.08	42	−0.01	−0.14
7	Me	H	Cl		−1.21	−1.03	48	−0.95	−0.81
8	Me	Ph	Cl		0.10	0.96	48	0.00	0.56
9	Me	H	Br		−0.96	−0.98	48	−0.93	−0.82
10	Et	Br	Br		0.29	−0.11	48	0.01	−0.08
11		H	OMe		−0.86	−0.22	44	−0.39	−0.14
12		Br	OMe		0.65	0.78	44	0.48	0.61
13		Ph	OMe		0.34	0.93	44	0.70	1.19
14	Me		OEt	1	−1.44	0.20	38	−1.18	0.28
15	Et		OEt	1	−1.34	0.11	38	−1.32	0.21
16	Pr		OEt	1	−1.13	0.32	38	−1.16	0.32
17	Me		OMe	1	−0.44	0.74	38	−0.63	0.58
18	Et		OMe	1	−0.82	0.29	38	−0.81	0.53
19	Pr		OMe	1	−0.83	0.82	38	−0.75	0.67
20	Me		OMe	2	−1.04	−0.19	38	−0.97	0.12
21	Et		OMe	2	−0.95	0.44	38	−1.07	0.06
22	Pr		OMe	2	−0.79	0.22	38	−0.98	0.19

[a] Calculated with model 1 in Table 4. [b] Calculated with model 2 in Table 4.

Table 2. Experimental and Calculated Relative Binding Affinity (pRA) at MT_1 and MT_2 Receptors for Antagonists

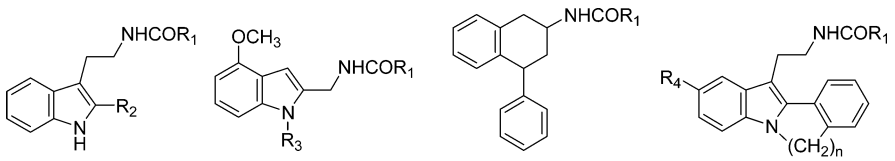

23-28 **29-32** **33-35** **36-56**

compd	R_1	R_2	R_3	R_4	*n*	pRA_1 (MT_1)	pRA_2 (MT_2)	ref	pRA_1 calcd[a]	pRA_2 calcd[b]
23	Me	Bn				−2.98	−1.73	48	−3.46	−1.55
24	Et	Bn				−3.08	−1.33	51	−3.29	−1.11
25	Me	*p*-Me-Bn				−3.83	−1.62	51	−3.75	−1.57
26	Me	*p*-OMe-Bn				−3.70	−1.74	51	−3.79	−1.64
27	cBu	H				−3.78	−3.09	48	−3.50	−3.27
28	cBu	Br				−3.26	−3.02	48	−3.41	−3.08
29	Et		Bn			−3.34	−1.43	45	−3.39	−1.57
30	Et		*p*-Cl-Bn			−3.65	−1.49	45	−3.57	−1.56
31	cBu		H			−3.26	−3.36	45	−3.24	−3.53
32	Et		H			−3.15	−3.01	45	−3.05	−2.83
33	Me					−2.69	−0.85	51	−2.70	−1.12
34	Et					−2.73	−0.92	51	−2.52	−0.63
35	CH_2Cl					−2.57	−0.69	51	−2.62	−0.92
36	Me			H	1	−2.47	−1.71	38	−2.37	−2.06
37	Et			H	1	−2.49	−1.71	38	−2.16	−1.41
38	cPr			H	1	−3.07	−2.83	38	−2.64	−2.37
39	cBu			H	1	−3.26	−3.53	38	−2.84	−3.20
40	cPr			OMe	1	−1.85	−0.46	38	−2.43	−0.66
41	cPr			OEt	1	−2.55	−1.22	38	−2.67	−1.48
42	Me			H	2	−2.77	−2.04	38	−2.63	−2.19
43	Et			H	2	−2.35	−1.45	38	−2.44	−1.69
44	cBu			H	2	−3.49	−3.03	38	−3.06	−3.12
45	cBu			OMe	2	−2.82	−2.99	38	−3.02	−2.19
46	Me			H	3	−2.56	−2.83	38	−2.59	−2.49
47	Et			H	3	−2.24	−2.14	38	−2.40	−1.97
48	cPr			H	3	−2.25	−2.20	38	−2.79	−2.43
49	cBu			H	3	−2.58	−2.97	38	−3.01	−3.32
50	Me			OMe	3	−2.62	−1.28	38	−2.52	−1.34
51	Et			OMe	3	−1.90	−0.63	38	−2.33	−0.80
52	cPr			OMe	3	−2.88	−1.56	38	−2.74	−1.43
53	cBu			OMe	3	−3.06	−1.98	38	−2.97	−2.23
54	Me			OEt	3	−2.89	−2.55	38	−2.83	−2.45
55	Et			OEt	3	−2.61	−1.82	38	−2.62	−1.92
56	cPr			OEt	3	−3.65	−2.41	38	−3.05	−2.53

[a] Calculated with model 3 in Table 4. [b] Calculated with model 4 in Table 4.

To test the reliability of our statistical results on both structure−affinity and structure−intrinsic activity relationships, we resynthesized and tested on cloned receptor subtypes the affinity and the intrinsic activity of some N-substituted MLT derivatives (**72**−**74**, Table 5). These compounds, which had been previously tested only on brain tissues expressing a heterogeneous population of receptors, are characterized by the presence of substituents of different shape and bulk, able, in our hypothesis, to modulate the selectivity and the intrinsic activity at the MLT MT_1 and MT_2 receptors. The experimental data were compared to those predicted by our 3D-QSAR models.

Results and Discussion

The compounds reported in Tables 1−3 were submitted to comparative molecular field analysis (CoMFA) in order to devise quantitative models for structure−affinity and structure−intrinsic activity relationships. The agonist compounds **1**−**22** (see Table 1), sharing the MLT substructure or its bioisosteric one (**11**−**13**), were superposed onto a minimum-energy conformation of MLT, formerly identified as one of the putatively active ones.[26,53] The antagonists **23**−**56** (see Table 2) were aligned maximizing the superposition of the benzene ring in the indole nucleus for compounds **23**−**32** and **36**−**56**, or in the tetralin nucleus for compounds **33**−**35**, of the amide group, and of the lipophilic fragment lying out of the plane of the above-mentioned aromatic ring. Two alignments were built corresponding to different conformations of the antagonist structures, having the last fragment on the same side as or opposite the acylaminoethyl chain of MLT derivatives (see Experimental Section for details). The two aligned data sets will be referred to as syn and anti, respectively. The same alignment rules were also applied to ligands **1**−**4**, **7**−**13**, **23**, **27**−**33**, and **57**−**71** (see Table 3) for structure−intrinsic activity studies.

We report and discuss the 3D-QSAR models obtained by applying the CoMFA steric field alone, for two reasons. First, in the sets of compounds included in the models, the structural variation was mainly steric, being generally due to alkyl or aryl groups or halogens. This led us to suppose that different 3D descriptors, such as electrostatic, lipophilic, or H-bond descriptors, could only introduce noise into the statistical models. In fact, the inclusion of the electrostatic field, in addition to the steric field, did not significantly improve the predictive power of the corresponding partial least squares (PLS) models. The best increment of Q^2 was of less than 0.05.

Table 3. Experimental and Calculated Relative Intrinsic Activity (IAr) at MT_1 and MT_2 Receptors for Ligands Selected for Structure−Intrinsic Activity Studies

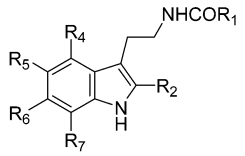

1-4, 7-10, 23, 27, 28, 57-69

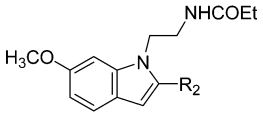

11-13, 70

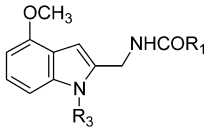

29-33, 71

compd	R_1	R_2	R_3	R_4	R_5	R_6	R_7	IAr_1 (MT_1)	IAr_2 (MT_2)	ref	IAr_1 calcd[a]	IAr_2 calcd[b]
1 (MLT)	Me	H		H	OMe	H	H	1.00	1.00		1.01	0.93
2	Me	Br		H	OMe	H	H	0.98	1.05	44	1.04	1.06
3	Me	I		H	OMe	H	H	1.00	1.02	44	1.05	1.07
4	Me	Ph		H	OMe	H	H	0.96	0.98	44	1.01	1.09
7	Me	H		H	Cl	H	H	0.99	1.00	48	0.81	0.88
8	Me	Ph		H	Cl	H	H	1.00	1.00	48	0.84	1.05
9	Me	H		H	Br	H	H	0.99	0.95	48	0.85	0.90
10	Et	Br		H	Br	H	H	1.01	1.00	48	0.97	1.05
11		H						0.93	1.03	44	0.97	1.07
12		Br						0.95	1.27	44	0.96	1.20
13		Ph						0.92	1.17	44	1.05	1.21
23	Me	Bn		H	H	H	H	−0.12	0.07	48	−0.02	0.18
27	cBu	H		H	H	H	H	0.16	0.10	48	0.18	0.20
28	cBu	Br		H	H	H	H	0.17	0.30	48	0.22	0.33
29	Et		Bn					0.03	0.18	45	−0.08	0.05
30	Et		*p*-Cl-Bn					0.04	0.01	45	−0.09	0.00
31	cBu		H					−0.01	0.26	45	0.01	0.20
32	Et		H					0.05	0.30	45	0.21	0.43
33	Me		H					0.08	0.42	45	0.22	0.45
57	Me	H		H	F	H	H	0.77	0.88	48	0.61	0.76
58	Me	H		H	OH	H	H	0.53	0.77	49, 56	0.74	0.84
59	Me	H		H	Me	H	H	0.79	0.85	48	0.86	0.91
60	cBu	H		H	Cl	H	H	0.46	0.20	48	0.43	0.34
61	cBu	Ph		H	Cl	H	H	0.52	0.65	48	0.46	0.54
62	Me	H		H	H	H	H	0.54	0.81	48	0.57	0.73
63	cBu	Ph		H	H	H	H	0.01	0.39	48	0.21	0.39
64	Me	H		OMe	H	H	H	0.61	0.63	43	0.57	0.73
65	Me	H		H	H	OMe	H	0.74	0.55	43	0.56	0.51
66	Me	H		H	H	H	OMe	0.77	0.58	43	0.61	0.47
67	Me	H		OMe	OMe	OMe	H	0.74	0.73	43	0.79	0.64
68	Me	H		H	OMe	Cl	H	0.96	1.00	55, 56	1.00	0.90
69	Me	H		H	OMe	H	OMe	0.98	0.62	43	1.04	0.65
70		$(CH_2)_2Ph$						0.75	0.27	44	0.65	0.30
71	Et		Ph					0.22	0.49	45	0.22	0.48

[a] Calculated with model 9 in Table 4. [b] Calculated with model 10 in Table 4.

Table 4. Statistics of the CoMFA Models

model	data set	dependent variable	alignment	receptor	SDy[a]	*N* [b]	LV	Q^2	SDEP	R^2	*s*
1	agonists[c]	pRA_1		MT_1	0.82	22	4	0.77	0.39	0.93	0.25
2	agonists[c]	pRA_2		MT_2	0.56	22	4	0.59	0.36	0.88	0.22
3	antagonists[d]	pRA_1	syn	MT_1	0.52	34	3	0.37	0.40	0.70	0.30
4	antagonists[d]	pRA_2	syn	MT_2	0.85	34	5	0.68	0.47	0.91	0.28
5	antagonists[d]	pRA_2-pRA_1	syn		0.78	34	3	0.55	0.51	0.78	0.39
6	antagonists[d]	pRA_1	anti	MT_1	0.52	34	4	0.41	0.39	0.79	0.25
7	antagonists[d]	pRA_2	anti	MT_2	0.85	34	5	0.59	0.53	0.87	0.34
8	antagonists[d]	pRA_2-pRA_1	anti		0.78	34	3	0.54	0.52	0.78	0.39
9	ligands[e]	IAr_1	syn	MT_1	0.39	34	3	0.74	0.20	0.92	0.11
10	ligands[e]	IAr_2	syn	MT_2	0.36	34	4	0.83	0.15	0.95	0.09
11	ligands[e]	IAr_1	anti	MT_1	0.39	34	4	0.77	0.18	0.95	0.10
12	ligands[e]	IAr_2	anti	MT_2	0.36	34	3	0.79	0.16	0.92	0.11

[a] Standard deviation of the dependent variable. [b] Number of compounds. [c] Compounds reported in Table 1. [d] Compounds reported in Table 2. [e] Compounds reported in Table 3.

Second, the CoMFA models obtained with the steric field alone were easier to interpret in terms of chemical modification of the reference structures. We also applied the CoMSIA steric, electrostatic, and lipophilic fields to the description of 3D properties, but no PLS model having significantly better predictive power was obtained. The statistical parameters of the CoMFA models with the steric field are reported in Table 4.

The data sets resulted from a deliberate selection of the structural variation available from the known ligands. In treating MLT receptor agonists (Table 1), we were mainly interested in studying the structure−

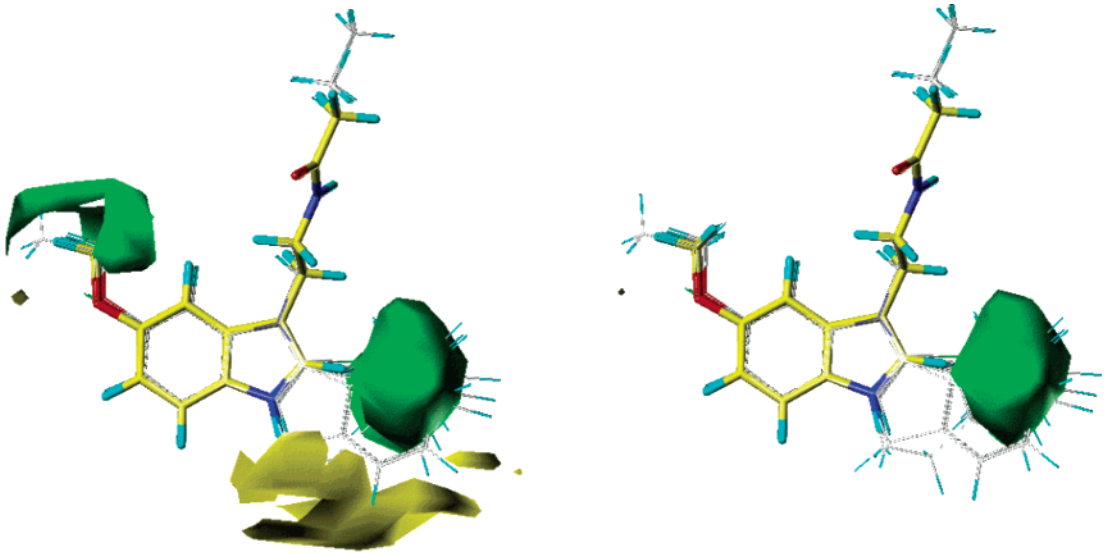

Figure 1. CoMFA standard deviation × coefficient contour plots for agonist compounds reported in Table 1 (models 1 and 2 in Table 4). The left contour plot refers to MT_1 and the right one to MT_2 affinity. The contour level is ±0.01. Steric occupancy of the green regions (positive coefficients) is correlated to an increase in binding affinity, and that of the yellow region (negative coefficients) is correlated to a decrease in binding affinity. Melatonin is represented as capped sticks with yellow carbons. The other compounds are represented by lines with conventional atom color coding.

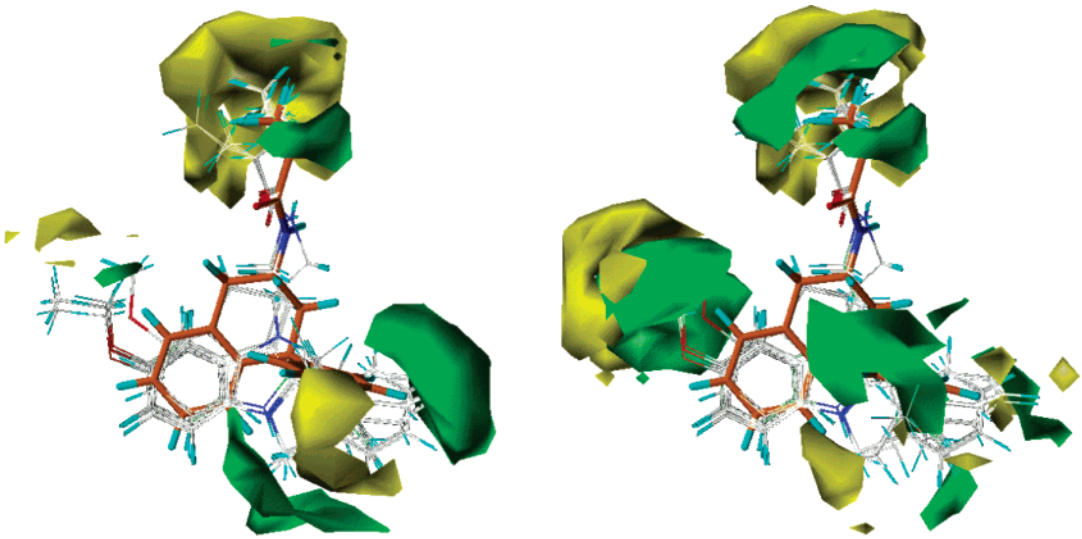

Figure 2. CoMFA standard deviation × coefficient contour plots for antagonists reported in Table 2, relative to the syn alignment (models 3 and 4 in Table 4). The left contour plot refers to MT_1 (contour level of ±0.003) and the right one to MT_2 affinity (contour level of ±0.006). Steric occupancy of the green regions (positive coefficients) is correlated to an increase in binding affinity, and that of the yellow regions (negative coefficients) is correlated to a decrease in binding affinity. 4P-PDOT (**34**) is represented as capped sticks with orange carbons. The other compounds are represented by lines with conventional atom color coding.

affinity relationship relative to the modulation of those positions corresponding to positions 1 and 2 of the indole ring of MLT. For this reason, we selected compounds with different structural features at these positions and with alkoxy groups or halogens at the position corresponding to position 5 of MLT, omitting known compounds having other substituents. The best CoMFA model obtained was a four-latent-variable one for both MT_1 and MT_2 receptor subtypes (models 1 and 2 in Table 4, respectively). The corresponding contour plots are represented in Figure 1, and the calculated relative affinity values (pRA) are reported in Table 1. As can be seen in Figure 1, substituents at position 2 of MLT enhance MT_1 binding affinity while the occupation of a region of space corresponding to that of the methylene groups between positions 1 and 2 of compound **14**−**22** is badly tolerated, as indicated by the yellow area under the steric positive green one. The agonists selected for the analysis had a limited variation in their MT_2 affinity, with a pRA standard deviation of 0.56 compared to 0.82 at the MT_1 receptor. For this reason, the statistical quality of the model developed for the MT_2 receptor is somewhat reduced and, in particular, because of its low predictive power, it can be exploited for qualitative considerations only. Within the cited limitation, the CoMFA model in Figure 1 shows a steric positive (green) region corresponding to position 2 of MLT, still due to the higher affinity of compounds with a substituent in this area. An additional binding interaction for substituents at this position had already been postulated[26] and a positive effect on affinity had been reported in different 3D-QSAR studies on binding data on tissues expressing a heterogeneous population of

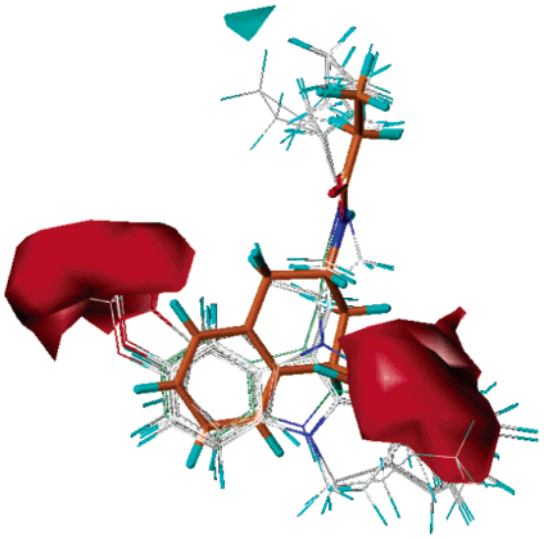

Figure 3. CoMFA standard deviation × coefficient contour plots for antagonists reported in Table 2, relative to the syn alignment (model 5 in Table 4). The contour level is ±0.006. The color codes are the following: (red) MT_2 selectivity; (cyan) MT_1 selectivity. 4P-PDOT (**34**) is represented as capped sticks with orange carbons. The other antagonists are represented by lines with conventional atom color coding.

receptors.[46,47] This positive effect was confirmed at both MT_1 and MT_2 receptor subtypes.

On the other hand, the requirements for receptor interaction at position 2 had already been reported in a study on 2-substituted indole MLT receptor ligands in which the substituents were selected to test the effect of their lipophilic, steric, and electronic properties on receptor affinity. In that study, agonist compounds had shown very similar behavior at both MT_1 and MT_2 subtypes, with lipophilicity being the major determinant for an increase in binding affinity.[44] This result is consistent with the CoMFA models now described, since the substituents at position 2 in the compounds considered in the present work are mainly lipophilic, and the steric field could therefore be representative of a lipophilic interaction with the binding site.

Substituents occupying the region spanning positions 1 and 2 of MLT are tolerated at the MT_2 receptor, giving no significant CoMFA coefficients, while the presence of steric bulk in the yellow region of Figure 1 lowers MT_1 affinity to a statistically significant extent. The length of the alkoxy group in the position corresponding to position 5 of MLT was not correlated to MT_1 or MT_2 affinity. The same was observed for the *N*-acyl chain substituents. This last result is in contrast with what is reported in previous 3D-QSAR studies,[41,46,47] where a positive effect on affinity was observed for propionyl and butiryl derivatives over the acetyl ones and a decrease of affinity was observed for bulkier alkoxy groups. Our results have to be attributed to the particular subset of agonists selected for the present structure−affinity study, where the overwhelming effect of the steric field at positions 1 and 2 led to smaller coefficients around the acyl chain and the 5-methoxy group. In the model for MT_1 affinity, a positive (green) region is observed that corresponds to the methyl fragment of the 5-methoxy group. This is due to the general lowering in affinity observed for the 5-halogen derivatives **7**−**10** with respect to the 5-methoxy ones, which is statistically more significant for MT_1 data.

As for the antagonist dataset, structure−affinity relationships were investigated for both the syn and anti alignments, obtaining PLS models with similar statistics (models 3−8 in Table 4) and equivalent contour plots. The graphical representation of the CoMFA coefficients in the following models refers to the syn alignment, as do the calculated pRA values in Table 2.

The pRA standard deviation at the MT_1 receptor was quite low, affecting the quality of the statistical parameters obtained (models 3 and 6 in Table 4) and the predictive power of the PLS models. In fact, MT_1 antagonists are characterized by a lower variation of affinity compared with MT_2 antagonists and it is possible to note that there are no potent MT_1 antagonists, while structural variation can give rise to significant improvement in MT_2 binding interactions.

In Figure 2, representing the CoMFA contour plots for MT_1 and MT_2 antagonists, it is possible to note that the lipophilic tails of the amide side chain yield similar effects at both MT_1 and MT_2 receptors for the compounds selected for the analysis. Small groups, such as the methyl or ethyl one, increase the binding affinity, while bulkier substituents, such as the cyclopropyl or the cyclobutyl ring, exert a negative effect, as can be seen from the green and yellow regions surrounding the amide side chain. The negative effect of bulky substituents at both receptor subtypes confirms what was observed by other authors considering ligands whose binding data were obtained from native tissues with a heterogeneous population of receptor subtypes.[36,46]

Steric occupancy in the region corresponding to position 5 of MLT influences binding to MT_1 and MT_2 receptors in different ways. In fact, MT_2 affinity is increased by the presence of the methoxy group, as indicated by the positive green region. In contrast, a bulkier ethoxy group causes a decrease in affinity, occupying the yellow negative region surrounding the green one. The affinity for the MT_1 receptor is less influenced by this modulation, as can be deduced by the absence of high coefficients in this region of space.

Moreover, MT_1 and MT_2 contour plots greatly differ in the regions surrounding positions 1 and 2 of MLT (lower right of the plots). In fact, MT_1 binding affinity is increased by the presence of a substituent in the position corresponding to position 2 of MLT, as indicated by the green region on the right of the contour plot. On the other hand, potency at the MT_2 receptor is enhanced by substituents positioned out of the plane of the indole (or tetralin), as can be seen from the green area covering the phenyl substituent of 4P-PDOT (**34**). The presence of steric bulk in this area has a moderate negative effect on MT_1 affinity, as indicated by the small yellow region in the corresponding area of the left image.

To further investigate the structural features affecting subtype selectivity, a 3D-QSAR analysis was performed using the difference in relative affinity at MT_1 and MT_2 receptors as the dependent variable. The graphical result of this analysis is reported in Figure 3, where the two red volumes refer to regions of space whose occupancy is correlated to selectivity for the MT_2 receptor. These are positioned around the methoxy group of indole derivatives and in the cited out-of-plane region.

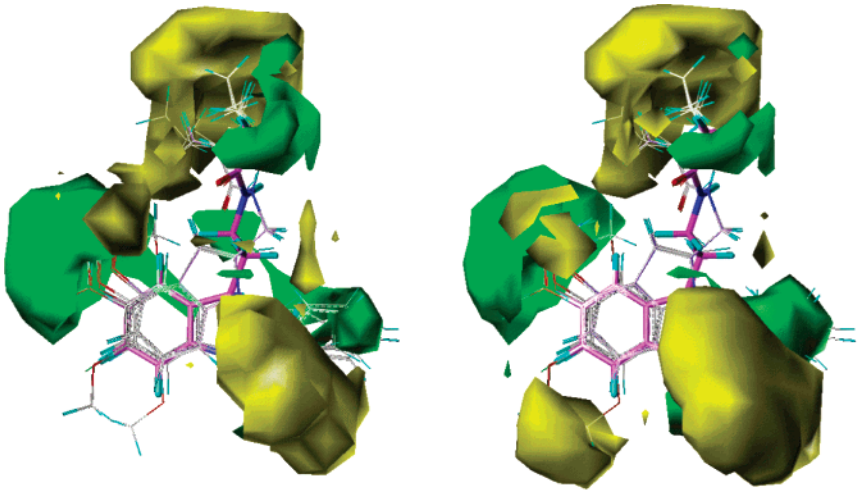

Figure 4. CoMFA standard deviation × coefficient contour plots for ligands reported in Table 3, relative to the syn alignment (models 9 and 10 in Table 4). The left contour plot refers to intrinsic activity at the MT_1 receptor, and the right one refers to that at the MT_2 receptor. The contour level is ±0.0012. Steric occupancy of the green regions (positive coefficients) is correlated to an increase in intrinsic activity, and that of the yellow region (negative coefficients) is correlated to a decrease in intrinsic activity. Luzindole (**23**) is represented as capped sticks with magenta carbons. The other compounds are represented by lines with conventional atom color coding.

The latter represents, in our opinion, the most relevant finding for selectivity and confirms our hypothesis of an additional pocket at the MT_2 binding site.

From a comparison of the results obtained from structure−affinity relationship studies at the two receptor subtypes for agonists and antagonists, it seems that the MT_2 receptor is characterized by a higher steric tolerance, in particular in the region of space surrounding positions 1 and 2 of the indole ring. While for the MT_2 receptor it was possible to define regions of space whose occupancy is related to selectivity toward this receptor subtype, this was not possible for the MT_1 receptor, given the unavailability of MT_1-selective compounds, but it was only possible to indicate regions of space whose occupancy is detrimental to MT_1 affinity.

Structure−intrinsic activity relationships were also investigated at both receptor subtypes to identify the features that characterize agonist and antagonist behavior. A set of ligands was selected (Table 3), composed by giving compounds whose intrinsic activity had been homogeneously evaluated by means of the GTPγS test on cloned receptors. Agonists, partial agonists, and antagonists were mutually aligned by superposing their common features (see Experimental Section). This alignment could be not consistent with their orientation at the active site of MT_1 and MT_2 receptors for two reasons. First, even if it is not known how these compounds interact at their binding site, it is possible that agonists would place their pharmacophore elements differently from antagonists to activate the receptor. Moreover, the occupancy of the out-of-plane pocket at the MT_2 receptor could affect the orientation of the antagonists at their binding site. On the other hand, this alignment was consistent with the aim of our study, a 3D-QSAR analysis revealing the structural features that can be correlated to differences in intrinsic activity at the two receptor subtypes.

The set of compounds exhibited a gradual change in the intrinsic activity values, shifting from agonist to partial agonist to antagonist behavior depending on the presence or the absence of certain structural features. The intrinsic activity values at the MT_1 and MT_2 receptors appeared to be quite well correlated to each other, and the requirements for receptor activation therefore seemed to be similar for the two receptor subtypes. The application of the CoMFA protocol provided analogous results for the two receptors, with differences mainly of a quantitative nature. Both the syn and anti alignments were analyzed, obtaining models that are comparable from a statistical point of view and for the information provided. The results of the PLS analysis are summarized in Table 4 (models 9−12). For the syn alignment, the calculated intrinsic activity values (IAr) are reported in Table 3 and the CoMFA contour plots are depicted in Figure 4. From this graphical representation, it is possible to note that a small group in the amide side chain increases the intrinsic activity, as shown by the presence of a positive green region. The same was observed for the regions corresponding to positions 2 and 5 of MLT. In contrast, a bulkier substituent in the side chain, such as the cyclobutyl ring, decreases the intrinsic activity at both receptor subtypes, moving the compounds toward the antagonist behavior. The same happens when the yellow area out of the plane of the molecules is occupied. An interpretation of this result may be that the presence of steric bulk in this yellow region is not allowed for an agonist at either of the receptor subtypes. As seen before, however, this bulk is tolerated at the MT_2 receptor if the compound behaves as an antagonist. The yellow area corresponding to positions 6 and 7 of MLT pertains exclusively to the MT_2 receptor: substituents occupying this area decrease the intrinsic activity at the MT_2 receptor. On the other hand, it had already been reported that substituents at these positions lead to a general decrease of affinity.[47] For 6-Cl-MLT (**68**), the observed pRA were −0.81 (MT_1)[55] and 0.02 (MT_2),[56] while 4,6-dimethoxyMLT (**67**) had pRA values of −3.68 (MT_1) and −2.91 (MT_2) and 7-methoxyMLT (**69**) had values of −2.78 (MT_1) and −3.33 (MT_2).[43]

The results of these structure−intrinsic activity relationships are in agreement with what was reported

Table 5. Binding Affinity and Intrinsic Activity of N-Substituted MLT Derivatives at MT_1 and MT_2 Receptor Subtypes

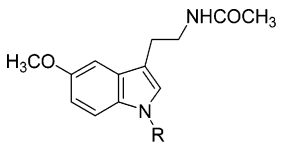

compd	R	pK_i(MT_1)	IAr(MT_1)	pK_i(MT_2)	IAr(MT_2)
1	H	9.78	1.00	9.53	1.00
72	Me	8.65	1.06	8.76	0.98
73	Ph	6.74	0.85	6.87	0.53
74	Bn	6.85	0.07	8.19	−0.09

Table 6. Prediction of Relative Affinity and Intrinsic Activity for MLT Receptor Agonists and Antagonists Belonging to the Series of N-Substituted MLT and Benzofuran Derivatives[a]

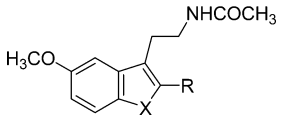

compd	X	R	pRA_1	pRA_2	IAr_1	IAr_2
72	*N*-Me	H	−0.55	−0.32	0.95[b]	0.96[b]
			−1.13	*−0.77*	*1.06*	*0.98*
74	*N*-Bn	H	−3.19[b]	−1.19[b]	0.51[b]	0.36[b]
			−2.93	*−1.34*	*0.07*	*−0.09*
75	O	Ph	0.97	0.95	0.97[b]	1.10[b]
			1.08[c]	*1.19*[c]	*agonist*[c]	*agonist*[c]
76	O	*m*-methoxy-Bn	−3.40[b]	−0.29[b]	0.43[b]	0.42[b]
			−2.53[c]	*−0.02*[c]	*antagonist*[c]	*antagonist*[c]

[a] The observed properties are reported in italics. [b] The predicted MT_1 and MT_2 values for intrinsic activity and for the relative affinity of the antagonists were calculated by the CoMFA models based on the syn alignment (models 9, 10, 3, and 4, respectively). [c] Reference 54.

for MLT receptor ligands described in the literature. In fact, the negative effect on intrinsic activity of bulky acylating groups was also observed on naphthalenic bioisosters of MLT,[36] as well as a lowering of intrinsic activity for 2-*N*-acylaminoalkylindoles due to the presence of a *N*-benzyl substituent occupying a region of space out of the plane of their indole ring.[45]

This set of compounds was also submitted to a structure−affinity relationship study, giving results that are in complete accordance with those obtained for agonists and antagonists treated separately (data not reported).

The findings derived from 3D-QSAR models on receptor subtype selectivity and intrinsic activity were validated through biological tests on MLT analogues. We resynthesized and tested on cloned receptor subtypes some N-substituted MLT derivatives (**72**−**74**), which had been previously tested only on brain tissues. In accordance with our CoMFA results, the different size and shape of the substituent at the nitrogen atom modulated binding affinity and intrinsic activity at the two receptor subtypes, as can be inferred from the biological data obtained and reported in Table 5. Compared to the *N*-methyl derivative **72**, a planar phenyl ring lowered the affinity at both receptors, while, interestingly, the benzyl group of **74** induced a complete loss of intrinsic activity but was well tolerated for MT_2 affinity, leading to some subtype selectivity. This can be explained by our findings, supposing that the benzyl group can be accommodated in the MT_2 lipophilic pocket out of the plane of the indole ring.

A class of benzofuran bioisosters of MLT has been recently reported[54] in which a substituted benzyl group in position 2 led to MT_2-selective antagonists, while a 2-phenyl substituent gave a potent agonist. Also in this case, the out-of-plane hindrance could be related to MT_2-selective antagonism.

The expected relative affinity and intrinsic activity values for the agonists and for the antagonists, in both series of N-substituted MLT (**72** and **74**) and benzofuran derivatives (**75** and **76**), were calculated with the appropriate CoMFA models and are reported in Table 6. The models based on the syn alignment were employed for antagonists and for all the intrinsic activity calculations.

The binding affinity values are properly predicted, even if only a qualitative agreement was observed for the agonist *N*-methyl-MLT (**72**) and for the antagonist *m*-methoxybenzylbenzofuran derivative (**76**). The intrinsic activity of the agonists **72** and **75** was correctly predicted, while intermediate intrinsic activity was predicted for the antagonists, probably due to an overestimation of the positive effect of the 5-methoxy group. In fact, our training set included no 5-substituted MLT derivative having very low intrinsic activity, although some of them have been reported in the literature,[38,51] because of the unavailability of GTPγS binding data.

Other questions about the conformation of ligands at their binding site cannot be addressed by the data available so far. These concern the orientation of the amide function, which is free to rotate in all the compounds considered, and the existence of models specular to those discussed. In fact, for each MLT conformation described, a specular one exists and, accordingly, specular alignments could be obtained either by inverting the torsional angles of achiral compounds or by employing the enantiomeric forms of the chiral ones. These questions can only be addressed by the design of rigid compounds with a fixed spatial arrangement of their pharmacophore elements and by the measurement of enantioselectivity of chiral compounds.

Conclusions

We analyzed the biological data available in the literature in search of the features that characterize MT_1/MT_2 subtype selectivity for compounds acting both as agonists and as antagonists, and we derived 3D-QSAR CoMFA models that accounted for the different binding affinity within selected series of compounds.

According to these models, subtype selectivity for MLT receptor agonists is related, at least partially, to the filling of a region of space between those occupied by substituents at positions 1 and 2 of the indole ring of MLT. On the other hand, 3D-QSAR models for antagonists allowed for the identification of two volumes whose occupancy can result in MT_2-selective receptor binding. In particular, the region of space out of the plane of the indole ring of MLT is also correlated to a decrease in intrinsic activity, and it is proposed as a key feature for the design of MT_2-selective antagonists, as

proved by the pharmacological behavior of N-substituted MLT derivatives.

Experimental Section

Chemistry. Compounds **72**−**74** were resynthesized according to the procedure described in ref 47.

Pharmacology. N-substituted MLT derivatives **72**−**74** were characterized by evaluating their binding affinity at MT_1 and MT_2 receptors and their in vitro functional activity.

Binding to h-MT_1 and h-MT_2 receptors was determined using 2-[^{125}I]-iodomelatonin (100 pM) as the labeled ligand in competition experiments on cloned human MT_1 and MT_2 receptors stably expressed in NIH3T3 rat fibroblast cells. The characterization of NIH3T3-MT_1 and MT_2 cells has already been described in detail.[55,56] pK_i values were calculated from IC_{50} values obtained from competition curves by the method of Cheng and Prussoff[57] and are the mean values of at least three independent determinations performed in duplicate. SEM of pK_i values were lower than 0.1.

The intrinsic activity of the compounds was evaluated on [^{35}S]-guanosine-5′-*O*-(3-thiotriphosphate) ([^{35}S]GTPγS) binding in NIH3T3cells stably transfected with human MT_1 or MT_2 receptors. The system provides a functional measurement for the interaction between melatonin receptors and pertussis toxin sensitive G proteins.

The detailed description and validation of this method have been reported elsewhere.[49,55,56]

In cell lines expressing human MT_1 or MT_2 receptors, MLT produced a concentration-dependent stimulation of basal [^{35}S]-GTPγS binding with a maximal stimulation, above basal levels, of 370% and 250% for MT_1 and MT_2 receptors, respectively. In the case of MLT analogues, the amount of bound [^{35}S]GTPγS is proportional to the level of the analogue-induced G-protein activation and is related to the intrinsic activity of the compounds. Full agonists increased the basal [^{35}S]GTPγS binding in a concentration-dependent manner, like the natural ligand MLT, whereas partial agonists increased it to a much lesser extent than that of MLT and antagonists were without effect. The relative intrinsic activity values (IAr) were obtained by dividing the maximum ligand-induced stimulation of [^{35}S]-GTPγS binding by that of MLT, as measured in the same experiment.

The interaction between ligands and melatonin was investigated by competition experiments in which increasing concentrations of an antagonist inhibit the maximum melatonin-induced stimulation of [^{35}S]GTPγS binding.

Compound Selection and Biological Variables. Agonists and antagonists (Tables 1 and 2, respectively) were selected among those compounds whose binding data at both cloned MT_1 and MT_2 receptor subtypes were available and whose agonist or antagonist behavior had been either evaluated in a pharmacological test or estimated by means of the GTPγS test. In particular, compounds whose IAr had been obtained by the GTPγS method were classified as agonists provided that their IAr values at the MT_1 and MT_2 receptors were both higher than 0.90; compounds were classified as antagonists when both their IAr values were lower than 0.30. Compounds not fulfilling these criteria were discarded. The other compounds were classified on the basis of their pharmacological profile, as reported in the literature.

The same set of agonists and of antagonists was used for structure−affinity relationship studies at MT_1 and MT_2 receptors.

Binding affinity was expressed as pRA, that is, the negative logarithm of relative affinity (RA) calculated as the pK_i of compound minus the pK_i of MLT under the same experimental conditions. This procedure was necessary to overcome the problem of the heterogeneity of binding data obtained under different experimental conditions, in particular from MT_1 and MT_2 receptors expressed in different cellular lines.

The pharmacological profile of compounds **5**, **6**, **14**−**22**, and **36**−**56** had been evaluated in the pigment aggregation response of *Xenopus laevis* melanophores, where an involvement of the Mel_{1c} receptor subtype has been supposed; however, some of these compounds, also tested on MT_1 and MT_2 receptors cloned in NIH3T3 cells, demonstrated the same agonist or antagonist action as in the melanophore assay.[38] Tetracyclic compounds **20**−**22** were classified as agonists, their reported IC_{50} values being more than 4000 times lower than their EC_{50} values.[38]

Compounds selected for structure−intrinsic activity studies (Table 3) were homogeneously tested at MT_1 and MT_2 receptor subtypes by means of the GTPγS method, as reported in the pharmacological section, and their relative intrinsic activity (IAr) was used as the dependent variable in the statistical analysis.

Molecular Modeling. Molecular modeling studies were performed with Sybyl 6.8[58] running on a Silicon Graphics O2 workstation. Molecules were built using the standard sketch procedure of Sybyl, and their geometries were optimized using the Tripos force field[59] with the Powell method[60] to an energy gradient of 0.01 kcal mol^{-1} Å^{-1}, ignoring the electrostatic contribution.

Only minimum energy conformations were considered throughout the studies.

Alignment Rules. Agonists were aligned on MLT, taken as the reference compound in one of its putative bioactive conformations obtained from our previous pharmacophore studies (model B in ref 26). The alignment was performed by means of a rigid fit procedure, superposing the four atoms of the amide function, the centroid of the benzene portion of the indole ring, and, when present, the oxygen atom of the alkoxy group onto those of MLT.

Two different alignments of antagonists were submitted to the CoMFA protocol, corresponding to the so-called syn and anti superposition models, as reported in ref 45. In fact, for those antagonists having a lipophilic substituent (generally, a phenyl ring) that can occupy a region of space out of the plane of their core aromatic nucleus, corresponding to the indole ring or the benzene portion of the tetralin ring, it is necessary to define the disposition of the substituent relative to that of the acylaminoethyl side chain of MLT derivatives. The syn alignment is characterized by the acylaminoethyl side chain and the out-of-plane substituent positioned on the same side, with respect to the plane of the core aromatic nucleus. The anti alignment is characterized by the two groups on opposite sides. 4P-PDOT (**34**) was used as the reference compound for the alignment, since it has limited conformational freedom. In particular, the cis isomer of 4P-PDOT (equatorial amide side chain and pseudoequatorial phenyl ring) was selected as the reference for the anti alignment, while its trans isomer (equatorial amide and pseudoaxial phenyl ring) was the reference for the syn alignment. On the other hand, the cis and trans isomers of 4P-PDOT can occupy a very similar region of space, with an analogous disposition of the features used for compound superposition.[45] The rigid fit alignment was based on the four atoms of the amide function, the centroid of the benzene portion of the tetralin or indole nucleus, and the centroid of the substituent positioned out of the plane of the molecule, when present, which were superposed onto those of 4P−PDOT.

Compounds selected for structure−intrinsic activity studies were aligned on luzindole (**23**), which was in the same conformation as in the antagonist dataset. The syn and anti alignments were obtained by means of a rigid fit procedure, superposing the four atoms of the amide function, the centroid of the benzene portion of the indole nucleus, and the centroid of the out-of-plane substituent, when present, onto those of luzindole.

3D-QSAR. The CoMFA module of Sybyl was applied to structure−affinity and structure−intrinsic activity studies. The CoMFA[61] steric and electrostatic fields and the CoMSIA[62,63] steric, electrostatic, and lipophilic fields were calculated within a lattice of 1 Å of grid resolution, whose extension was at least 4 Å beyond every molecular boundary in each direction, applying an sp^3 carbon atom with a point charge of +1 as the probe atom. The electrostatic field was calculated from Gasteiger−Hückel charges,[64,65] with a dielec-

tric function dependent on $1/r$. For those points where the steric cutoff was reached, the drop electrostatic option was enabled. This corresponds to fixing the electrostatic potential to the mean of all the nonexcluded electrostatic values calculated at the same grid point, in practice excluding the point from the analysis. Regression analyses were performed applying the partial least squares (PLS) algorithm[66] in Sybyl; the steric field alone and the combination of the steric and electrostatic fields were used as structural descriptors to evaluate their correlation with affinity (pRA) and intrinsic activity (IAr) data.

The optimal number of latent variables was defined by means of the cross-validation technique[67] on the basis of the Q^2 value calculated with the SAMPLS algorithm.[68] The standard deviation of error in prediction[69] was calculated as $\mathrm{SDEP} = [\sum(y - y_{\mathrm{PRED}})^2/N]^{1/2}$. The number of latent variables giving the highest Q^2 value was selected, provided that the last latent variable would give an increment of Q^2 of at least 0.03. If this did not happen, the last latent variable was not considered, since the increase of model complexity was not counterbalanced by an adequate improvement in the quality of the model. No energy filter was applied to the final non-cross-validated analyses.

References

(1) Cassone, V. M. Effects of melatonin on vertebrate circadian system. *Trends Neurosci.* **1990**, *13*, 457−464.

(2) Shochat, T.; Haimov, I.; Lavie, P. Melatonin—the key to the gate of sleep. *Ann. Med.* **1998**, *30*, 109−114.

(3) Pang, S. F.; Li, L.; Ayre, E. A.; Pang, C. S.; Lee, P. P. N.; Xu, R. K.; Chow, P. H.; Yu, Z. H.; Shiu, S. Y. W. Neuroendocrinology of melatonin in reproduction: recent developments. *J. Chem. Neuroanat.* **1998**, *14*, 157−166.

(4) Doolen, S.; Krause, D. N.; Dubocovich, M. L.; Duckles, S. P. Melatonin mediates two distinct responses in vascular smooth muscle. *Eur. J. Pharmacol.* **1998**, *345*, 67−69.

(5) Arangino, S.; Cagnacci, A.; Angiolucci, M.; Vacca, A. M.; Longu, G.; Volpe, A.; Melis, G. B. Effects of melatonin on vascular reactivity, catecholamine levels, and blood pressure in healthy men. *Am. J. Cardiol.* **1999**, *83*, 1417−1419.

(6) Motilva, V.; Cabeza, J.; Alarcón de la Lastra, C. New issues about melatonin and its effects on the digestive System. *Curr. Pharm. Des.* **2001**, *7*, 909−931.

(7) Nowak, J. Z.; Zawilska, J. B. Melatonin and its physiological and therapeutic properties. *Pharm. World Sci.* **1998**, *20*, 18−27.

(8) Wetterberg, L. Melatonin and clinical application. *Reprod., Nutr., Dev.* **1999**, *39*, 367−382.

(9) Li, P.-K.; Witt-Enderby, P. A. Melatonin receptors as potential targets for drug discovery. *Drugs Future* **2000**, *25*, 945−957.

(10) Reiter, R. J.; Tan, D. X.; Cabrera, J.; D'Arpa, D.; Sainz, R. M.; Mayo, J. C.; Ramos, S. The oxidant/antioxidant network: role of melatonin. *Biol. Signals Recept.* **1999**, *8*, 56−63.

(11) Lipartiti, M.; Franceschini, D.; Zanoni, R.; Gusella, M.; Giusti, P.; Cagnoli, C. M.; Kharlamov, A.; Manev, H. Neuroprotective effects of melatonin. *Adv. Exp. Med. Biol.* **1996**, *398*, 315−321.

(12) Nelson, R. J.; Drazen, D. L. Melatonin mediates seasonal adjustments in immune function. *Reprod., Nutr., Dev.* **1999**, *39*, 383−398.

(13) Liu, R. Y.; Zhou, J. N.; van Heerikhuize, J.; Hofman, M. A.; Swaab, D. F. Decreased melatonin levels in postmortem cerebrospinal fluid in relation to ageing, Alzheimer's desease, and apolipoprotein E-epsilon4/4 genotype. *J. Clin. Endocrinol. Metab.* **1999**, *84*, 323−327.

(14) Nosjean, O.; Ferro, M.; Cogé, F.; Beauverger, P.; Henlin, J.-M.; Lefoulon, F.; Fauchère, J.-L.; Delagrange, P.; Canet, E.; Boutin, J. A. Identification of the melatonin-binding site MT3 as the quinone reductase 2. *J. Biol. Chem.* **2000**, *275*, 31311−31317.

(15) Smirnov, A. N. Nuclear Melatonin Receptors. *Biochemistry (Moscow)* **2001**, *66*, 19−26.

(16) Paz Romero, M.; García-Pergañeda, A.; Guerrero, J. M.; Osuna, C. Membrane-bound calmodulin in Xenopus Laevis oocytes as a novel binding site for melatonin. *FASEB J.* **1998**, *12*, 1401−1408.

(17) Sugden, D.; Chong, N. W. S.; Lewis, D. F. V. Structural requirements at the melatonin receptor. *Br. J. Pharmacol.* **1995**, *114*, 618−623.

(18) Grol, C. J.; Jansen, J. M. The high affinity melatonin binding site probed with conformationally restricted ligands—II. Homology modeling of the receptor. *Bioorg. Med. Chem.* **1996**, *4*, 1333−1339.

(19) Navajas, C.; Kokkola, T.; Poso, A.; Honka, N.; Gynther, J.; Laitinen, J. T. A rhodopsin-based model for melatonin recognition at its G protein-coupled receptor. *Eur. J. Pharmacol.* **1996**, *304*, 173−183.

(20) Conway, S.; Canning, S. J.; Barrett, P.; Guardiola-Lemaitre, P.; Delagrange, P.; Morgan, P. J. The roles of valine 208 and histidine 211 in ligand binding and receptor function of the ovine $Mel_{1a\beta}$ melatonin receptor. *Biochem. Biophys. Res. Commun.* **1997**, *239*, 418−423.

(21) Conway, S.; Mowat, E. S.; Drew, J. E.; Barrett, P.; Delagrange, P.; Morgan, P. J. Serine residues 110 and 114 are required for agonist binding but not antagonist binding to the melatonin MT_1 receptor. *Biochem. Biophys. Res. Commun.* **2001**, *282*, 1229−1236.

(22) Nelson, C. S.; Ikeda, M.; Gompf, H. S.; Robinson, M. L.; Fuchs, N. K.; Yoshioka, T.; Neve, K. A.; Allen, C. N. Regulation of melatonin 1a receptor signaling and trafficking by asparagine-124. *Mol. Endocrinol.* **2001**, *15*, 1306−1317.

(23) Dubocovich, M. L.; Yun, K.; Al-Ghoul, W. M.; Benloucif, S.; Masana, M. I. Selective MT2 melatonin receptor antagonists block melatonin-mediated phase advances of circadian rhythms. *FASEB J.* **1998**, *12*, 1211−1220.

(24) Hunt, A. E.; Al-Ghoul, W. M.; Gillitte, M. U.; Dubocovich, M. L. Activation of MT2 melatonin receptors in rat suprachiasmatic nucleus phase advances the circadian clock. *Am. J. Physiol.: Cell Physiol.* **2001**, *280*, C110−C118.

(25) Drazen, D. L.; Nelson, R. J. Melatonin receptor subtype MT2 (Mel1b) and not mt1 (Mel1a) is associated with melatonin-induced enhancement of cell-mediated and humoral immunity. *Neuroendocrinology* **2001**, *74*, 178−184.

(26) Spadoni, G.; Balsamini, C.; Diamantini, G.; Di Giacomo, B.; Tarzia, G.; Mor, M.; Plazzi, P. V.; Rivara, S.; Lucini, V.; Nonno, R.; Pannacci, M.; Fraschini, F.; Stankov, B. M. Conformationally restrained melatonin analogs: synthesis, binding affinity for the melatonin receptor, evaluation of the biological activity, and molecular modeling study. *J. Med. Chem.* **1997**, *40*, 1990−2002.

(27) Tarzia, G.; Diamantini, G.; Di Giacomo, B.; Spadoni, G.; Esposti, D.; Nonno, R.; Lucini, V.; Pannacci, M.; Fraschini, F.; Stankov, B. M. 1-(2-Alkanamidoethyl)-6-methoxyindole derivatives: a new class of potent indole melatonin analogs. *J. Med. Chem.* **1997**, *40*, 2003−2010.

(28) Copinga, S.; Tepper, P. G.; Grol, C. J.; Horn, A. S.; Dubocovich, M. L. 2-Amido-8-methoxytetralins: a series of nonindolic melatonin-like agents. *J. Med. Chem.* **1993**, *36*, 2891−2898.

(29) Depreux, P.; Lesieur, D.; Mansour, H. A.; Morgan, P.; Howell, H. E.; Renard, P.; Caignard, D. H.; Pfeiffer, B.; Delagrange, P.; Guardiola, B.; Yous, S.; Demarque, A.; Adam, G.; Andrieux, J. Synthesis and structure−activity relationships of novel naphthalenic and bioisosteric related amidic derivatives as melatonin receptor ligands. *J. Med. Chem.* **1994**, *37*, 3231−3239.

(30) Sugden, D. *N*-Acyl-3-amino-5-methoxychromans: a new series of non-indolic melatonin analogues. *Eur. J. Pharmacol.* **1994**, *254*, 271−275.

(31) Langlois, M.; Brémont, B.; Shen, S.; Poncet, A.; Andrieux, J.; Sicsic, S.; Serraz, I.; Mathé-Allainmat, M.; Renard, P.; Delagrange, P. Design and synthesis of new naphthalenic derivatives as ligands for 2-[^{125}I]iodomelatonin binding sites. *J. Med. Chem.* **1995**, *38*, 2050−2060.

(32) Mathé-Allainmat, M.; Gaudy, F.; Sicsic, S.; Dangy-Caye, A.-L.; Shen, S.; Bremont, B.; Benatalah, Z.; Langlois, M.; Renard, P.; Delagrange, P. Synthesis of 2-amido-2,3-dihydro-1*H*-phenalene derivatives as new conformationally restricted ligands for melatonin receptors. *J. Med. Chem.* **1996**, *39*, 3089−3095.

(33) Garratt, P. J.; Travard, S.; Vonhoff, S.; Tsotinis, A.; Sugden, D. Mapping the melatonin receptor. 4. Comparison of the binding affinities of a series of substituted phenylalkyl amides. *J. Med. Chem.* **1996**, *39*, 1797−1805.

(34) Li, P.-K.; Chu, G.-H.; Gillen, M. L.; Witt-Enderby, P. A. Synthesis and receptor binding studies of quinolinic derivatives as melatonin receptor ligands. *Bioorg. Med. Chem. Lett.* **1997**, *7*, 2177−2180.

(35) Davies, D. J.; Garratt, P. J.; Tocher, D. A.; Vonhoff, S.; Davies, J.; Teh, M. T.; Sugden, D. Mapping the melatonin receptor. 5. Melatonin agonists and antagonists derived from tetrahydrocyclopent[*b*]indoles, tetrahydrocarbazoles and hexahydrocyclohept-[*b*]indoles. *J. Med. Chem.* **1998**, *41*, 451−467.

(36) Leclerc, V.; Fourmaintraux, E.; Depreux, P.; Lesieur, D.; Morgan, P.; Howell, H. E.; Renard, P.; Caignard, D. H.; Pfeiffer, B.; Delagrange, P.; Guardiola-Lemaitre, B.; Andrieux, J. Synthesis and structure−activity relationships of novel naphthalenic and bioisosteric related amidic derivatives as melatonin receptor ligands. *Bioorg. Med. Chem.* **1998**, *6*, 1875−1887.

(37) Charton, I.; Mamai, A.; Bennejean, C.; Renard, P.; Howell, E. H.; Guardiola-Lemaître, B.; Delagrange, P.; Morgan, P. J.; Viaud, M.-C.; Guillaumet, G. Substituted oxigenated heterocycles and thio-analogues: synthesis and biological evaluation as melatonin ligands. *Bioorg. Med. Chem.* **2000**, *8*, 105−114.

(38) Faust, R.; Garratt, P. J.; Jones, R.; Yeh, L.-K.; Tsotinis, A.; Panoussopoulou, M.; Calogeropoulou, T.; Teh, M.-T.; Sugden, D. Mapping the melatonin receptor. 6. Melatonin agonists and antagonists derived from 6*H*-isoindolo[2,1-*a*]indoles, 5,6-dihydroindolo[2,1-*a*]isoquinolines, and 6,7-dihydro-5*H*-benzo[*c*]azepino[2,1-*a*]indoles. *J. Med. Chem.* **2000**, *43*, 1050−1061.

(39) Jellimann, C.; Mathé-Allainmat, M.; Andrieux, J.; Kloubert, S.; Boutin, J. A.; Nicolas, J.-P.; Bennejean, C.; Delagrange, P.; Langlois, M. Synthesis of phenalene and acenaphthene derivatives as new conformationally restricted ligands for melatonin receptors. *J. Med. Chem.* **2000**, *43*, 4051−4062.

(40) Jansen, J. M.; Copinga, S.; Gruppen, G.; Molinari, E. J.; Dubocovich, M. L.; Grol, C. J. The high affinity melatonin binding site probed with conformationally restricted ligands—I. Pharmacophore and minireceptor models. *Bioorg. Med. Chem.* **1996**, *4*, 1321−1332.

(41) Marot, C.; Chavatte, P.; Morin-Allory, L.; Viaud, M. C.; Guillaumet, G.; Renard, P.; Lesieur, D.; Michel, A. Pharmacophoric search and 3D-QSAR comparative molecular field analysis studies on agonists of melatonin sheep receptors. *J. Med. Chem.* **1998**, *41*, 4453−4465.

(42) Teh, M. T.; Sugden, D. Comparison of the structure−activity relationships of melatonin receptor agonists and antagonists: lengthening the *N*-acyl side-chain has differing effects on potency on *Xenopus* melanophores. *Naunyn-Schmiedeberg's Arch. Pharmacol.* **1998**, *358*, 522−528.

(43) Spadoni, G.; Mor, M.; Tarzia, G. Structure−affinity relationships of indole-based melatonin analogs. *Biol. Signals Recept.* **1999**, *8*, 15−23.

(44) Mor, M.; Spadoni, G.; Di Giacomo, B.; Diamantini, G.; Bedini, A.; Tarzia, G.; Plazzi, P. V.; Rivara, S.; Nonno, R.; Lucini, V.; Pannacci, M.; Fraschini, F.; Stankov, B. M. Synthesis, pharmacological characterization and QSAR studies on 2-substituted indole melatonin receptor ligands. *Bioorg. Med. Chem.* **2001**, *9*, 1045−1057.

(45) Spadoni, G.; Balsamini, C.; Diamantini, G.; Tontini, A.; Tarzia, G.; Mor, M.; Rivara, S.; Plazzi, P. V.; Nonno, R.; Lucini, V.; Pannacci, M.; Fraschini, F.; Stankov, B. M. 2-*N*-Acylaminoalkylindoles: design and quantitative structure−activity relationship studies leading to MT2-selective melatonin antagonists. *J. Med. Chem.* **2001**, *44*, 2900−2912.

(46) Sicsic, S.; Serraz, I.; Andrieux, J.; Brémont, B.; Mathé-Allainmat, M.; Poncet, A.; Shen, S.; Langlois, M. Three-dimensional quantitative structure−activity relationship of melatonin receptor ligands: a comparative molecular field analysis study. *J. Med. Chem.* **1997**, *40*, 739−748.

(47) Mor, M.; Rivara, S.; Silva, C.; Bordi, F.; Plazzi, P. V.; Spadoni, G.; Diamantini, G.; Balsamini, C.; Tarzia, G.; Fraschini, F.; Lucini, V.; Nonno, R.; Stankov, B. M. Melatonin receptor ligands: Synthesis of new melatonin derivatives and comprehensive comparative molecular field analysis (CoMFA) study. *J. Med. Chem.* **1998**, *41*, 3831−3844.

(48) Spadoni, G.; Balsamini, C.; Bedini, A.; Carey, A.; Diamantini, G.; Di Giacomo, B.; Tontini, A.; Tarzia, G.; Nonno, R.; Lucini, V.; Pannacci, M.; Stankov, B. M.; Fraschini, F. *N*-Acyl-5- and -2,5-substituted tryptamines: synthesis, activity and affinity for human mt_1 and MT_2 melatonin receptors. *Med. Chem. Res.* **1998**, *8*, 487−498.

(49) Spadoni, G.; Balsamini, C.; Bedini, A.; Diamantini, G.; Di Giacomo, B.; Tontini, A.; Tarzia, G.; Mor, M.; Plazzi, P. V.; Rivara, S.; Nonno, R.; Pannacci, M.; Lucini, V.; Fraschini, F.; Stankov, B. M. 2-[*N*-Acylamino(C_1−C_3)alkyl]indoles as MT1 melatonin receptor partial agonists, antagonists, and putative inverse agonists. *J. Med. Chem.* **1998**, *41*, 3624−3634.

(50) Nosjean, O.; Nicolas, J.-P.; Klupsch, F.; Delagrange, P.; Canet, E.; Boutin, J. A. Comparative pharmacological studies of melatonin receptors: MT1, MT2 and *MT*3/QR2. Tissue distribution of *MT*3/QR2. *Biochem. Pharmacol.* **2001**, *61*, 1369−1379.

(51) Dubocovich, M. L.; Masana, M. I.; Iacob, S.; Sauri, D. M. Melatonin receptor antagonists that differentiate between the human Mel_{1a} and Mel_{1b} recombinant subtypes are used to assess the pharmacological profile of the rabbit retina ML_1 presynaptic heteroreceptor. *Naunyn-Schmiedeberg's Arch. Pharmacol.* **1997**, *355*, 365−375.

(52) Rivara, S.; Mor, M.; Spadoni, G.; Tarzia, G.; Vacondio, F.; Lucini, V.; Plazzi, P. V. QSAR and 3D-QSAR characterization of MT2 selective melatonin receptor antagonists. Presented at the Hungarian−German−Italian−Polish Joint Meeting on Medicinal Chemistry, Budapest, Hungary, September 2−6, 2001.

(53) Jelliman, C.; Lefas-Le Gall, M.; Mathé-Allainmat, M.; Andrieux, J.; Sicsic, S.; Nicolas, J. P.; Boutin, J.; Delagrange, P.; Bennejan, C.; Renard, P.; Langlois, M. Design, sinthesis and biological evaluation of new melatoninergic compounds. Presented at the XVIth International Symposium on Medicinal Chemistry, Bologna, Italy, September 18−22, 2000; Poster PB98.

(54) Wallez, V.; Durieux-Poissonnier, S.; Chavatte, P.; Boutin, J. A.; Audinot, V.; Nicolas, J.-P.; Bennejean, C.; Delagrange, P.; Renard, P.; Lesieur, D. Synthesis and structure−affinity−activity relationships of novel benzofuran derivatives as MT_2 melatonin receptor selective ligands. *J. Med. Chem.* **2002**, *45*, 2788−2800.

(55) Nonno, R.; Lucini, V.; Pannacci, M.; Mazzucchelli, C.; Angeloni, D.; Fraschini, F.; Stankov, B. M. Pharmacological characterization of the human melatonin Mel1a receptor following stable transfection into NIH3T3 cells. *Br. J. Pharmacol.* **1998**, *124*, 485−492.

(56) Nonno, R.; Pannacci, M.; Lucini, V.; Angeloni, D.; Fraschini, F.; Stankov, B. M. Ligand efficacy and potency at recombinant human MT2 melatonin receptors: evidence for agonist activity of some mt1-antagonists. *Br. J. Pharmacol.* **1999**, *127*, 1288−1294.

(57) Cheng, Y. C.; Prussoff, W. H. Relation between the inhibition constant (Ki) and the concentration of inhibitor which causes fifty percent inhibition (IC_{50}) of an enzymatic reaction. *Biochem Pharmacol.* **1973**, *22*, 3099−3108.

(58) *Sybyl*, version 6.8; Tripos Inc. (1699 South Hanley Rd): St. Louis, MO 63144; 2001.

(59) Clark, M.; Cramer, R. D., III; Van Opdenbosch, N. Validation of the general purpose Tripos 5.2 force field. *J. Comput. Chem.* **1989**, *10*, 982−1012.

(60) Powell, M. J. D. Restart procedures for the conjugate gradient method. *Math. Program.* **1977**, *12*, 241−254.

(61) Cramer, R. D., III; Patterson, D. E.; Bunce, J. D. Comparative molecular field analysis (CoMFA). 1. Effect of shape on binding of steroids to carrier proteins. *J. Am. Chem. Soc.* **1988**, *110*, 5959−5967.

(62) Klebe, G.; Abraham, U.; Mietzner, T. Molecular Similarity Indices in a Comparative Analysis (CoMSIA) of Drug Molecules To Correlate and Predict Their Biological Activity. *J. Med. Chem.* **1994**, *37*, 4130−4146.

(63) Klebe, G.; Abraham, U. Comparative Molecular Similarity Index Analysis (CoMSIA) To Study Hydrogen-Bonding Properties and To Score Combinatorial Libraries. *J. Comput.-Aided Mol. Des.* **1999**, *13*, 1−10.

(64) Gasteiger, J.; Marsili, M. Iterative partial equalization of orbital electronegativity—Rapid access to atomic charges. *Tetrahedron* **1980**, *36*, 3219−3228.

(65) Hückel, Z. Quanten theoretische beiträge zum benzolproblem. I. Die electron enkonfiguration des benzols. *Z. Phys.* **1931**, *70*, 203−286.

(66) Wold, S.; Ruhe, A.; Wold, H.; Dunn, W. J. The covariance problem in linear regression. The partial least squares (PLS) approach to generalized inverses. *SIAM J. Sci. Stat. Comput.* **1984**, *5*, 735−743.

(67) Cramer, R. D., III; Bunce, J. D.; Patterson, D. E. Crossvalidation, bootstrapping, and partial least squares compared with multiple regression in conventional QSAR studies. *Quantum Struct.−Act. Relat.* **1988**, *7*, 18−25.

(68) Bush, B. L.; Nachbar, R. B. Sample-distance partial least squares: PLS optimized for many variables, with application to CoMFA. *J. Comput.-Aided Mol. Des.* **1993**, *7*, 587−619.

(69) Cruciani, G.; Clementi, S.; Baroni, M. Variable selection in PLS analysis. In *3D QSAR in Drug Design. Theory Methods and Applications*; Kubinyi, H., Ed.; ESCOM: Leiden, The Netherlands, 1993; p 552.

JM020982D